

# Hydrogen Bonding Effects on the Reorganization Energy for Photoinduced Charge Separation Reaction between Porphyrin and Quinone Studied by Nanosecond Laser Flash Photolysis

Tomoaki Yago,\* Masao Gohdo, and Masanobu Wakasa

Department of Chemistry, Graduate School of Science and Engineering, Saitama University,  
255 Shimo-okubo, Sakura-ku, Saitama, 338-8570, Japan

Received: October 16, 2009; Revised Manuscript Received: January 11, 2010

Alcohol concentration dependences of photoinduced charge separation (CS) reaction of zinc tetraphenylporphyrin (ZnTPP) and duroquinone (DQ) were investigated in benzonitrile by a nanosecond laser flash photolysis technique. The photoinduced CS reaction was accelerated by the addition of alcohols, whereas the addition of acetonitrile caused little effect on the CS reactions. The simple theory was developed to calculate an increase in reorganization energies induced by the hydrogen bonding interactions between DQ and alcohols using the chemical equilibrium constants for the hydrogen bonding complexes through the concerted pathway and the stepwise one. The experimental results were analyzed by using the Marcus equation where we took into account the hydrogen bonding effects on the reorganization energy and the reaction free energy for the CS reaction. The observed alcohol concentration dependence of the CS reaction rates was well explained by the formation of the hydrogen bonding complexes through the concerted pathway, demonstrating the increase in the reorganization energy by the hydrogen bonding interactions.

## Introduction

Hydrogen bonding plays an important role in a variety of biological electron transfer (ET) systems encompassing photosynthesis and respiration.<sup>1–5</sup> In biological ET systems, hydrogen bonding often modulates redox activities of ET cofactor molecules, fixing them to the appropriate positions in order to achieve the efficient energy conversions. In the photosynthetic reaction center of *Rhodobacter sphaeroides*, for example, differences in the redox activities between the two electron acceptor quinones are provided by the difference in the strength of hydrogen bonding with the amino acid residues from the protein environments.<sup>6</sup> According to the Marcus theory, the activation barrier for the ET reaction depends on the reaction free energy ( $\Delta G$ ) and the reorganization energy ( $\lambda$ ).<sup>7,8</sup> Electrochemical studies have shown that quinone and flavin anions are stabilized by the formation of intermolecular and intramolecular hydrogen bonding, suggesting the change of  $\Delta G$  for the ET reactions.<sup>9–15</sup> Fukuzumi et al. reported that the stabilizations of the charge separated states through hydrogen bonding between quinones and ammonium cations accelerates charge separation (CS) reactions in solutions.<sup>16</sup> The effects of hydrogen bonding on the ET reactions have been discussed with the proton-coupled ET reactions, which are also important in the biological systems.<sup>5,17–22</sup> In the proton-coupled ET reactions, the proton transfer increases  $\lambda$  as well as the stabilization of the charge separated state created by the ET reactions. Hydrogen bonding influences the configuration of the proton and then affects the ET reactions indirectly. The major role of hydrogen bonding in the biological ET reactions, which are not accompanied by the proton transfer, has been thought to be only the stabilization of the charge separated states so far.

Recent time-resolved electron paramagnetic resonance (EPR) studies on radical ion pairs generated by photoinduced CS

reactions suggested that the  $\lambda$  values are also increased by quinone anion–alcohol hydrogen bonding in polar solvents.<sup>23</sup> The solvent reorganization energies were found to be larger by ca. 0.2 eV than the predictions of the Marcus continuum dielectric model when the ET systems involved the hydrogen bonding complexes formed by the electron acceptor of quinone and alcohols. The results were supported by the molecular dynamics simulation<sup>24</sup> and quantum mechanical calculations<sup>25</sup> where the realistic molecular structures and interactions were taken into account. In those studies, however, the hydrogen bonding effects on the ET reaction rates have not been observed directly. Therefore, the kinetic study which includes the hydrogen bonding effects on  $\Delta G$  and  $\lambda$  is highly desirable to clarify the role of hydrogen bonding in the biological ET systems.

In this report, we studied photoinduced CS reactions accompanied by the formation of quinone–alcohol hydrogen bonding complexes in polar solvent by using a nanosecond laser flash photolysis. The photoinduced CS reaction between the photoexcited triplet state of zinc tetraphenylporphyrin (ZnTPP) and duroquinone (DQ) was accelerated by the addition of alcohols in benzonitrile (PhCN). The one-electron reduction potential of DQ was shifted to the positive direction due to the formation of the hydrogen bonding complexes between DQ and alcohols, indicating the decrease in  $\Delta G$  for the CS reactions. The theoretical analysis to examine the hydrogen bonding effects on  $\lambda$  is performed for the concerted ET pathway and the stepwise one using the chemical equilibrium constants for the hydrogen bonding complexes. Under the framework of the Marcus theory, the results indicate that the hydrogen bonding formation increases  $\lambda$  in addition to the decrease in  $\Delta G$ , resulting in the modulation of the CS reaction via the concerted pathway in the present ET system.

\* Corresponding author. Phone: +81-48-858-3094. Fax: +81-48-858-3382. E-mail: yago@chem.saitama-u.ac.jp.

## Experimental Section

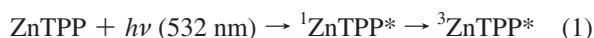
**Materials.** DQ (Sigma-Aldrich) was recrystallized twice from ethanol. ZnTPP was prepared by metalation of the corresponding free-base tetraphenylporphyrin and recrystallized twice from dichloromethane/methanol.<sup>26</sup> Methanol (MeOH, Cica, HPLC-grade), ethanol (EtOH, Cica, HPLC-grade), 1-propanol (1-PrOH, Cica), acetonitrile (AN, Cica, HPLC grade), and PhCN (Sigma-Aldrich, HPLC-grade) were used as received. Tetrabutylammonium hexafluorophosphate (TBAPF<sub>6</sub>, Fluka, 99%) was used as received.

**Nanosecond Laser Flash Photolysis.** Laser flash photolysis experiments were carried out with an apparatus that was essentially the same as an apparatus described elsewhere.<sup>27</sup> The second harmonic (532 nm) of a nanosecond Nd:YAG laser (Quanta-Ray, INDY; 7 ns fwhm) was used as an excitation light source. The excitation light was introduced perpendicularly to the monitoring light. The transient absorption was recorded by a digitizing oscilloscope (LeCroy, WavePro 960) with a photomultiplier tube (Hamamatsu, R636). The concentrations of ZnTPP and DQ were  $1 \times 10^{-4}$  and  $1\text{--}20 \times 10^{-4}$  mol dm<sup>-3</sup>, respectively. All experiments were carried out with argon-bubbled solutions at 296 K.

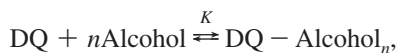
**Cyclic Voltammetry.** Cyclic voltammetry (CV) measurements were performed with a three-electrode potentiostat system (Cypress systems, model CS-1090) consisting of a platinum working electrode and a reference electrode of an Ag wire in a fitted tube containing  $1 \times 10^{-2}$  mol dm<sup>-3</sup> of AgNO<sub>3</sub> in  $1 \times 10^{-1}$  mol dm<sup>-3</sup> of tetrabutylammonium perchlorate/AN. TBAPF<sub>6</sub> ( $1 \times 10^{-1}$  mol dm<sup>-3</sup>) was used as an electrolyte. Scan rates were 10–100 mV s<sup>-1</sup>. The concentration of ZnTPP and DQ in PhCN was  $1 \times 10^{-3}$  mol dm<sup>-3</sup>. Ferricenium ion/ferrocene (Fc<sup>+</sup>/Fc) was used as an internal standard. Solutions containing samples and electrolyte were deoxygenated by nitrogen bubbling for 15 min prior to measurements. All experiments were performed at 296 K.

## Results

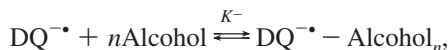
**Reaction Scheme.** The previous time-resolved EPR study showed that the photoinduced CS reaction proceeds between the photoexcited triplet state of ZnTPP and DQ in PhCN.<sup>28</sup> In the PhCN solution, the semiquinone radical of DQ is not produced even in the presence of the alcohols used in the present study.<sup>23c</sup> We can therefore describe the photoinduced CS reaction in the present system as follows:



where  ${}^1\text{ZnTPP}^*$ ,  ${}^3\text{ZnTPP}^*$ ,  $\text{ZnTPP}^{+\bullet}$ , and  $\text{DQ}^{-\bullet}$  represent the excited singlet and triplet states of ZnTPP, ZnTPP cation radical, and DQ anion radical, respectively. The formations of hydrogen bonding between quinone anions and protic solvents have been reported from the EPR measurements,<sup>29</sup> density functional calculations,<sup>30</sup> and electrochemical studies.<sup>10–14</sup> Thus, DQ and  $\text{DQ}^{-\bullet}$  can form the hydrogen bonding complexes with alcohols in PhCN.<sup>11,23c</sup> The chemical equilibria for the DQ–alcohol hydrogen bonding complexes are represented as



$$K = \frac{[\text{DQ} - \text{Alcohol}_n]}{[\text{DQ}][\text{Alcohol}]^n} \quad (3)$$



$$K^- = \frac{[\text{DQ}^{-\bullet} - \text{Alcohol}_n]}{[\text{DQ}^{-\bullet}][\text{Alcohol}]^n} \quad (4)$$

Here,  $K$  and  $K^-$  are the chemical equilibrium constants of the hydrogen bonding complexes for DQ and  $\text{DQ}^{-\bullet}$ , respectively.  $n$  is the number of alcohol molecules participating in the one hydrogen bonding complex. In eqs 3 and 4, the chemical equilibria for the hydrogen bonding complexes are approximately treated with the single global equilibrium constants.

**Alcohol Concentration Dependences of Photoinduced CS Reaction.** Figure 1 shows transient absorption spectra observed at delay times of 0.1, 2, and 5  $\mu\text{s}$  after laser excitation of ZnTPP ( $1 \times 10^{-4}$  mol dm<sup>-3</sup>) in the presence of DQ ( $2 \times 10^{-3}$  mol dm<sup>-3</sup>) in PhCN containing no alcohols. A transient absorption peak due to the triplet–triplet (T–T) absorption of  ${}^3\text{ZnTPP}^*$  was observed at 470 nm.<sup>31,32</sup> DQ concentration dependence of the time profile of the transient absorption ( $A(t)$ ) was observed at 470 nm. The decay of the  $A(t)$  curve at 470 nm was accelerated by increasing the DQ concentration. In the presence of DQ,  $A(t)$  curves had a fast decay component and an almost constant one. From the spectral data reported previously, the fast component can be assigned to the decay of the T–T absorption of  ${}^3\text{ZnTPP}^*$  and the almost constant one to the transient absorption of  $\text{ZnTPP}^{+\bullet}$  and  $\text{DQ}^{-\bullet}$  produced by the photoinduced CS reactions.<sup>33,34</sup> We first investigated the DQ concentration dependences of the decay rate constants ( $k$ ) of  ${}^3\text{ZnTPP}^*$  at 470 nm in the presence of the various concentrations of MeOH. Figure 2 shows examples of DQ concentration dependences of  $k$  observed in the absence and presence of MeOH (0.2 and 0.3 mol dm<sup>-3</sup>). The pseudo-first-order rate constants increased by linearly increasing the concentration of DQ. The second-order rate constants of the photoinduced CS reactions ( $k_q$ ) were evaluated from the slopes of these plots. The determined  $k_q$  value for each MeOH concentration was

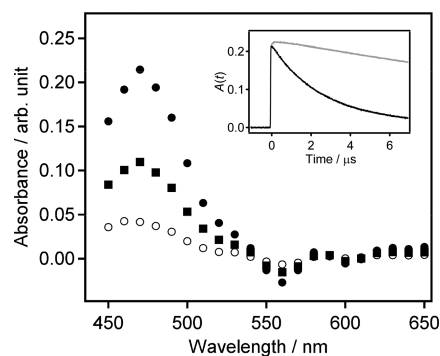


**Figure 1.** Transient absorption spectra observed at delay times of 0.1 (filled circles), 2 (filled squares), and 5  $\mu\text{s}$  (empty circles) after laser excitation of ZnTPP ( $1 \times 10^{-4}$  mol dm<sup>-3</sup>) in the presence of DQ ( $2 \times 10^{-3}$  mol dm<sup>-3</sup>) in PhCN. The spectra were measured in the absence of alcohols. The inset shows a time profile of transient absorption ( $A(t)$ ) observed at 470 nm in the absence of (gray line) and in the presence of DQ ( $2 \times 10^{-3}$  mol dm<sup>-3</sup>).

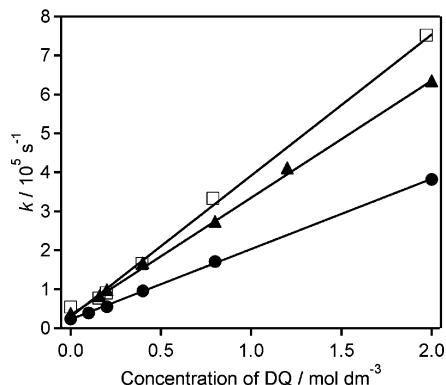


**Figure 2.** DQ concentration dependences of decay rate ( $k$ ) observed for the T–T absorption of ZnTPP ( $1 \times 10^{-4}$  mol dm $^{-3}$ ) in the absence of MeOH (filled circles) and in the presence of MeOH: 0.2 mol dm $^{-3}$  (filled triangles) and 0.3 mol dm $^{-3}$  of MeOH (empty squares), respectively.

**TABLE 1: Rate Constants ( $k_q$ ) of Photoinduced Charge Separation Reactions from  $^3\text{ZnTPP}^*$  to DQ in PhCN in the Presence of MeOH, EtOH, 1-PrOH, and AN Obtained by Nanosecond Laser Flash Photolysis**

alcohol or AN	[alcohol] or [AN]/mol dm $^{-3}$	$k_q/10^8$ s $^{-1}$
MeOH	0.00	1.88
	0.05	2.25
	0.10	2.37
	0.15	2.60
	0.20	2.93
	0.24	3.26
	0.30	3.45
	0.37	3.44
EtOH	0.45	3.51
	0.10	2.71
	0.25	3.33
	0.50	3.74
1-PrOH	0.75	4.07
	0.13	2.47
	0.25	2.88
	0.5	3.27
AN	0.75	3.53
	0.34	2.07
	0.63	2.05
	1.00	2.10

listed in Table 1. The  $k_q$  values are smaller than the reaction rate constant for the diffusion controlled reactions ( $5.3 \times 10^9$  mol dm $^{-3}$  s $^{-1}$ ), indicating that the rate-determining step for the present photochemical reaction is CS and not the encounter process of the donor and acceptor molecules promoted by the diffusion motions. With the steady-state approximation,  $k_q$  is represented as follows:<sup>35</sup>

$$\frac{1}{k_q} = \frac{1}{k_{\text{dif}}} + \frac{1}{k_{\text{CS}}} \quad (5)$$

where  $k_{\text{dif}}$  and  $k_{\text{CS}}$  are the diffusion rate constant and the rate constant of the CS reaction in the ZnTPP\*–DQ complex, respectively. Figure 3a shows the MeOH concentration dependence of  $k_{\text{CS}}$  for the ZnTPP–DQ system in PhCN determined with eq 5 and the parameters of  $k_{\text{dif}} = 5.3 \times 10^9$  mol dm $^{-3}$  s $^{-1}$ . The value of  $k_{\text{dif}}$  was estimated from the relation of  $k_{\text{dif}} = 8k_{\text{B}}T/3\eta$  with the viscosity ( $\eta$ ) of PhCN ( $\eta = 1.2$  cP).<sup>36</sup> The CS reaction was accelerated by the addition of MeOH, and the acceleration was nearly saturated when the concentration of MeOH was higher than 0.3 mol dm $^{-3}$ . For comparison, the

similar measurements were performed by using AN instead of MeOH. The results obtained with AN are also plotted in Figure 3d. As can be seen in Figure 3d, the addition of AN has little effect on  $k_{\text{CS}}$  when the concentration of AN is lower than 1 mol dm $^{-3}$ . Since the dielectric constant ( $\epsilon$ ) and  $\eta$  of MeOH ( $\epsilon = 32.7$ ,  $\eta = 0.59$  cP)<sup>36</sup> and of AN ( $\epsilon = 35.9$ ,  $\eta = 0.34$  cP)<sup>36</sup> are similar, the results clearly indicate that the specific hydrogen bonding interactions between DQ and MeOH accelerate the photoinduced CS reactions in the present ET system. We have also observed accelerations of the CS reactions in the presence of EtOH and of 1-PrOH, as listed in Table 1. The feature of the alcohol concentration dependence of  $k_{\text{CS}}$  is varied with alcohols, as can be seen in Figure 3.

**One-Electron Reduction Potential of DQ under Varied Concentrations of Alcohol.** In the present study, the  $\Delta G$  values were evaluated from the following equation:<sup>37</sup>

$$\Delta G = E_{1/2}^{\text{ox}} - E_{1/2}^{\text{red}} - \frac{e^2}{\epsilon r} - E(T_1) \quad (6)$$

Here,  $E_{1/2}^{\text{red}}$ ,  $E_{1/2}^{\text{ox}}$ , and  $E(T_1)$  are the reduction potentials of DQ, the oxidation potential of ZnTPP, and the energy of  $^3\text{ZnTPP}^*$ , respectively. The term  $e^2/\epsilon r$  is the Coulomb attraction energy for the radical pairs at distance  $r$  where the CS reactions take place. To obtain the  $\Delta G$  value, we measured the cyclic voltammograms (CVs) of ZnTPP and DQ in the absence and presence of alcohols. Figure 4 shows MeOH concentration dependences of the CV observed for (a) DQ and (b) ZnTPP in PhCN, respectively. The  $E_{1/2}^{\text{red}}$  and  $E_{1/2}^{\text{ox}}$  values were determined from the midpoint between the cathodic and anodic peak potentials. The potential  $E_{1/2}^{\text{red}}$  for DQ was shifted to the positive direction with increasing MeOH concentration. The  $E_{1/2}^{\text{red}}$  values obtained in the absence and presence of (a) MeOH and (b) 1-PrOH, respectively, are shown in Figure 5. In each case,  $E_{1/2}^{\text{red}}$  for DQ was shifted to the positive direction with increasing alcohol concentration. The alcohol concentration dependences of  $E_{1/2}^{\text{red}}$  for quinones have been interpreted by the stabilization of the quinone anion due to the formation of the quinone anion–alcohol hydrogen bonding complexes.<sup>10–14</sup> On the other hand, the oxidation potential  $E_{1/2}^{\text{ox}}$  for ZnTPP $^{+*}$  was unchanged even in the presence of 1.0 mol dm $^{-3}$  of MeOH, indicating no specific interactions between ZnTPP and alcohols. The constant value of  $E_{1/2}^{\text{ox}} = +0.31$  V vs Fc $^+$ /Fc was used to estimate  $\Delta G$  throughout in this study.

In the absence of the alcohols,  $\Delta G$  is estimated to be  $-0.05$  eV from the measured values of  $E_{1/2}^{\text{red}} = -1.29$  V vs Fc $^+$ /Fc for DQ and  $E_{1/2}^{\text{ox}} = +0.31$  V vs Fc $^+$ /Fc for ZnTPP, the reported value of  $E(T_1) = 1.53$  eV,<sup>38</sup> and the calculated value of 0.12 eV for the Coulomb attraction energy with  $r = 5$  Å and  $\epsilon = 25.2$ <sup>36</sup> in PhCN. The alcohol concentration dependences of  $\Delta G$  originate from the shift of  $E_{1/2}^{\text{red}}$  for DQ due to the formation of the hydrogen bonding complexes. The shift of  $E_{1/2}^{\text{red}}$  is given as a function of the alcohol concentration in accordance with the Nernst equation as follows:<sup>39</sup>

$$E_{1/2}^{\text{red}} = E_{1/2}^{\text{redo}} + \frac{RT}{F} \ln \left( \frac{1 + K^- [\text{Alcohol}]^n}{1 + K [\text{Alcohol}]^n} \right) \quad (7)$$

where  $E_{1/2}^{\text{redo}}$  is the reduction potential of DQ in the absence of alcohols.

## Discussion

The rates of the ET reactions are well-described by the Marcus equation. The observed alcohol concentration depend-

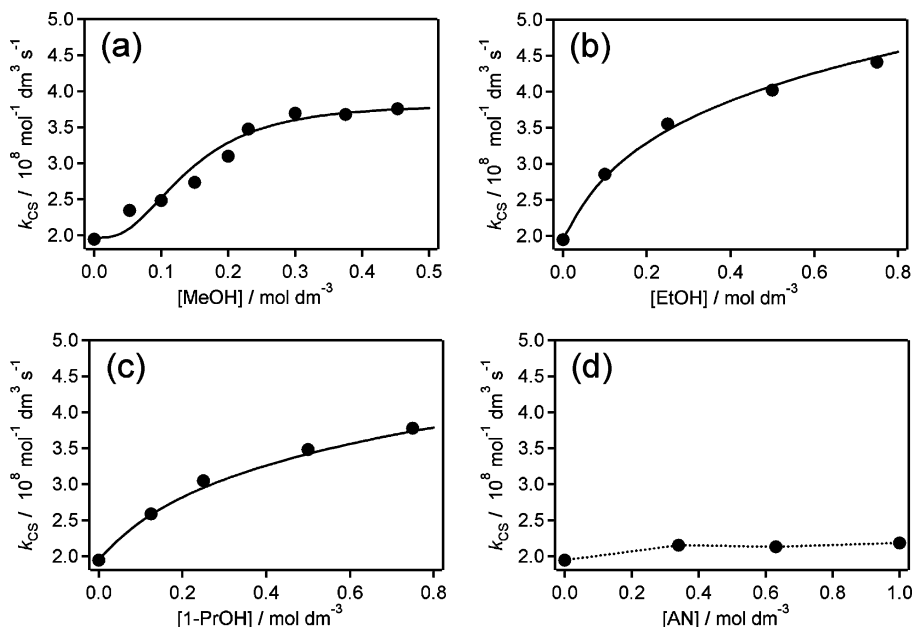


**Figure 3.** Plots of the rate constant ( $k_{CS}$ ) for the CS reaction in the  $^3\text{ZnTPP}^*\text{--DQ}$  complex versus the concentrations of (a) MeOH, (b) EtOH, (c) 1-PrOH, and (d) AN in PhCN. Solid lines show  $k_{CS}$  calculated with the Marcus equation where the hydrogen bonding effects on  $\Delta G$  and  $\lambda$  are taken into account with the concerted ET pathway.

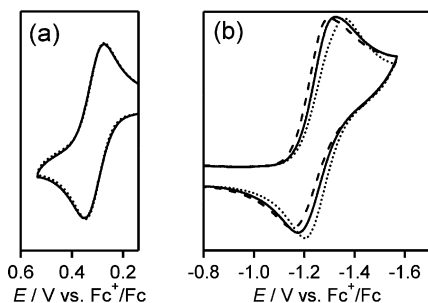


**Figure 4.** Cyclic voltammograms of (a) ZnTPP observed in the absence (solid line) and in the presence of  $1 \text{ mol dm}^{-3}$  of MeOH (dotted line) in PhCN and (b) DQ observed in PhCN in the absence of MeOH (dotted line) and in the presence of MeOH:  $0.2 \text{ mol dm}^{-3}$  (solid line) and  $0.34 \text{ mol dm}^{-3}$  of MeOH (dashed line), respectively.

ences of  $k_{CS}$  were analyzed with the following classical Marcus equation:<sup>35</sup>

$$k_{CS} = Z \exp \left\{ -\frac{(\Delta G + \lambda)^2}{4\lambda k_B T} \right\} \quad (8)$$

where  $Z$  is a pre-exponential factor. The variable parameters in eq 8 are  $Z$ ,  $\Delta G$ , and  $\lambda$ . Among these parameters, we could assume that the  $Z$  value was constant in the present study. EtOH and 1-PrOH have similar viscosities ( $\eta = 1.08 \text{ cP}$  for EtOH and  $\eta = 1.94 \text{ cP}$  for 1-PrOH)<sup>36</sup> with PhCN ( $\eta = 1.24 \text{ cP}$ ).<sup>36</sup> Also, the addition of  $1 \text{ mol dm}^{-3}$  of AN, which has the lowest viscosity ( $\eta = 0.34 \text{ cP}$ )<sup>36</sup> in the solvents used, has little effect on  $k_{CS}$ , as can be seen in Figure 3. The diffusion motions of the solute molecules were not perturbed by the addition of the alcohols in the present alcohol concentrations. The parameters affected by the addition of alcohols are  $\Delta G$  and  $\lambda$ . In the previous study, we demonstrated that the alcohol concentration dependence of  $k_{CS}$  was not explained by the change of  $\Delta G$  alone.<sup>40</sup> We have proposed the increase in  $\lambda$  with the addition of alcohol in the present photoinduced CS reaction system. However, the mechanism on the increase in  $\lambda$  with the addition

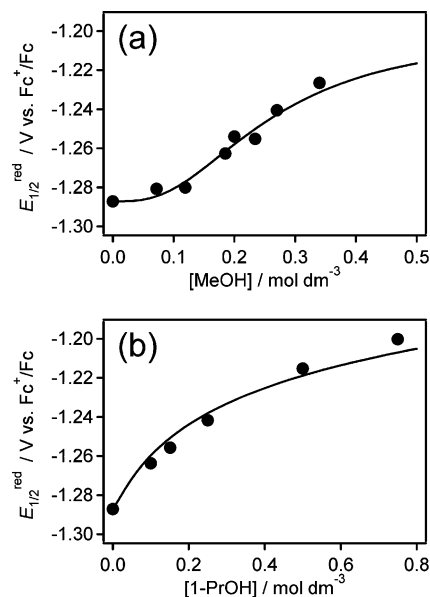


**Figure 5.** (a) MeOH and (b) 1-PrOH concentration dependences of  $E_{1/2}^{\text{red}}$  for DQ obtained by the cyclic voltammogram measurements in PhCN. Solid lines show fitting with the Nernst equation.

of alcohols has not been clarified yet. In the following, we have performed a theoretical analysis on the hydrogen bonding effects on  $\lambda$ , which accounts for the alcohol concentration dependences of  $k_{CS}$  observed.

**Calculations of Hydrogen Bonding Effects on  $\lambda$  with Chemical Equilibrium Constants.** Figure 6 shows a schematic representation of the energy surfaces for the neutral reactant and the charge separated product states plotted against the normalized reaction coordinate.<sup>41</sup> The solid lines denote the energy surfaces with the effects of the hydrogen bonding complexes, and the dashed lines indicate the energy surfaces in the absence of the hydrogen bonding complexes. The reactant state has the chemical equilibrium constant  $K$  for the formations of the hydrogen bonding complexes, while the product state has the constant of  $K^-$ . The chemical equilibrium is changed



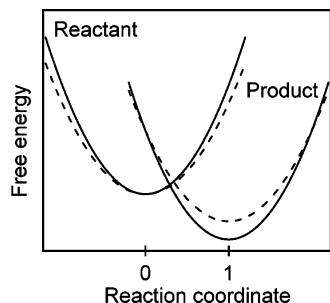
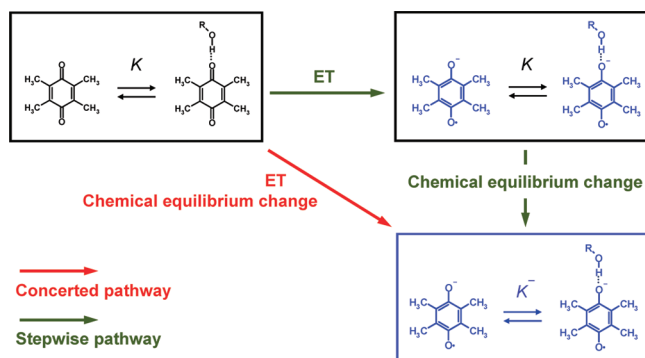


**Figure 6.** Schematic representation of the free energy surfaces for the neutral reactant with the charge separated product states plotted against the normalized reaction coordinate. The solid lines and dashed lines indicate the energy surfaces in the absence of and presence of the hydrogen bonding interactions, respectively.

### SCHEME 1: Concerted versus Stepwise Pathway Dichotomy in the Presence of Hydrogen Bonding Complexes



during the ET reactions in addition to the change of the solute molecule structures and of the solvent molecule polarizations. The charge separated state is stabilized by the formation of hydrogen bonding, resulting in the decrease of  $\Delta G$  for the CS reactions. At the equilibrium reaction coordinate for the product state, the reactant state is destabilized by the hydrogen bonding interactions because of the difference in the chemical equilibria among the reactant and product states. Similarly, the product state is also destabilized at the equilibrium reaction coordinate for the reactant state. These destabilizations of the reactant and product states give the hydrogen bonding effects on  $\lambda$  and always increase the  $\lambda$  values. The increases in  $\lambda$  due to the noncovalent bonding interactions were previously calculated using the chemical equilibrium constants.<sup>42</sup> Though the previous model provided the first interpretation for the increase in  $\lambda$  observed by time-resolved EPR spectroscopy, quantitative improvements are necessary to account for the alcohol concentration dependence of  $k_{\text{CS}}$  observed in the present study. Also, the concept of the concerted pathway and the stepwise pathway which are currently interested in the ion-coupling and proton-coupling ET reactions is not considered in the previous model.

When the third components are introduced in the ET reaction systems such as ion and proton, whole reactions take place, either the concerted pathway or stepwise one.<sup>20–22,43</sup> The concerted versus stepwise pathway dichotomy in the presence of the hydrogen bonding complexes is depicted in Scheme 1. Several theoretical models have been developed for those pathways in the ion-pairing and proton-coupling ET reactions where the correlations between the ET systems and the third components are strong.<sup>20–22,43</sup> The hydrogen bonding interactions between quinone anion and alcohols are relatively weak compared with the ion-coupling and proton-coupling interac-

tions. Here, the increase in  $\lambda$  due to hydrogen bonding is calculated for the concerted pathway and the stepwise one, respectively, using chemical equilibrium constants for the hydrogen bonding complexes.

In the concerted pathway, the chemical equilibrium is always maintained during the ET reactions. The necessary condition for the concerted pathway is that the formation/dissociation of the hydrogen bonding complexes is much faster than the ET process. Thus, the change of the chemical equilibrium is balanced with the virtual change of the charge distribution on the solute molecules. The  $\lambda$  which is defined as a minimum reversible work to stabilize the transition state<sup>7</sup> is therefore given by the stabilization energy of the quinone anion radical due to the hydrogen bonding complex formation. Fukuzumi et al. also reached a similar conclusion from the observation of the metal cation effects on the CS reactions involving quinone anions. The increase in  $\lambda$  is accompanied by a decrease in  $\Delta G$  due to the complex formation of quinone anions with the metal cations.<sup>44</sup> Analogous to the Nernst equation, the  $\lambda$  is derived from the integration of the infinitesimal works with the virtually constant compositions of the system<sup>45</sup> and can be written with  $K$  and  $K^-$  as follows:

$$\lambda = \lambda^{\circ} + \left| RT \ln \left( \frac{1 + K^- [\text{Alcohol}]^n}{1 + K [\text{Alcohol}]^n} \right) \right| \quad (9)$$

where  $\lambda^{\circ}$  is the reorganization energy in the absence of the hydrogen bonding interactions. To ensure the increase in  $\lambda$  by the hydrogen bonding interactions, we take the absolute values for the second term in eq 9. We refer the hydrogen bonding induced reorganization component in eq 9 to a *static* reorganization component. In the concerted pathway, the hydrogen bonding interaction does not affect the term  $(\Delta G + \lambda)$  in eq 8 due to the cancellation of the hydrogen bonding effect on  $\Delta G$  by that on  $\lambda$ . The hydrogen bonding effects only increase the denominator of the index in the exponential function in eq 8. As a result, the CS reaction is accelerated by the hydrogen bonding interactions in the Marcus normal region and also in the Marcus inverted region. We emphasize that the use of eq 9 to estimate the increase in  $\lambda$  due to hydrogen bonding is limited to the ET system where the ET reaction is sufficiently slower than the rate for the formation/dissociation of the hydrogen bonding complexes.

In the stepwise pathway, the ET reaction is faster than the formation/dissociation of the hydrogen bonding complexes. The ET reaction first takes place; then, the chemical equilibrium change occurs as a reorganization of the ET. The composition change of the chemical species during the ET reaction directly gives the new reorganization component in addition to the *static* reorganization component. We refer this new reorganization component to a *dynamical* reorganization component. In the previous study, the effects of formation/dissociation of the noncovalent bonding on  $\lambda$  were also calculated by using the chemical equilibrium constants for the noncovalent bonding complexes.<sup>42</sup> The calculated  $\lambda$  was purely derived from the instantaneous changes in the compositions of the chemical species during the ET events. The  $\lambda$  calculated in the previous study therefore corresponds to the *dynamical* reorganization component. The resultant  $\lambda$  in the stepwise pathway is given by

$$\lambda = \lambda^0 + \left| RT \ln \left( \frac{1 + K^- [\text{Alcohol}]^n}{1 + K [\text{Alcohol}]^n} \right) \right| + RT \ln \left( \frac{K^- [\text{Alcohol}]^n}{K [\text{Alcohol}]^n} \right) dn \quad (10a)$$

$$dn = \frac{K^- [\text{Alcohol}]^n}{1 + K^- [\text{Alcohol}]^n} - \frac{K [\text{Alcohol}]^n}{1 + K [\text{Alcohol}]^n} \quad (10b)$$

Here, the second term on the right-hand side of eq 10a represents the *dynamical* reorganization component. In the stepwise mechanism, the increase in  $\lambda$  induced by the hydrogen bonding interactions is larger than the stabilization energy for the charge separated state. The hydrogen bonding effects on  $k_{\text{CS}}$  become rather complex and both acceleration and deceleration of CS reactions occurs, depending on the strength of hydrogen bonding.

Contrary to the CS reactions, the hydrogen bonding effects on  $\Delta G$  and  $\lambda$  in the term  $(\Delta G + \lambda)$  in eq 8 do not cancel out for the charge recombination reactions in both pathways. The charge recombination reaction is strongly decelerated in the Marcus normal region and is accelerated in the Marcus inverted region by the effect of the hydrogen bonding interactions in both pathways.

**Comparison with the Experimental Data.** In the ET system used in the present study, the formation/dissociation of the hydrogen bonding complexes is faster than the CS process because of the slow CS reactions and the low concentration of DQ compared with the alcohol concentration. Therefore, the observed alcohol concentration dependences of  $k_{\text{CS}}$  in the present study are analyzed with the concerted pathway. In the analysis on the MeOH and 1-PrOH concentration dependences of  $k_{\text{CS}}$  and  $E_{1/2}^{\text{red}}$ , the chemical equilibrium constants of  $K$  and  $K^-$  are used as fitting parameters, while the other parameters were treated as constants. For the EtOH concentration dependence of  $k_{\text{CS}}$ , the reported chemical equilibrium constants ( $K \approx 0$  (mol dm<sup>-3</sup>)<sup>-1.3</sup> and  $K^- = 85$  (mol dm<sup>-3</sup>)<sup>-1.3</sup>)<sup>11</sup> are used. The constant parameters used are  $Z = 5 \times 10^{11}$  mol<sup>-1</sup> dm<sup>3</sup> s<sup>-1</sup>,<sup>40</sup>  $\lambda^0 = 0.9$  eV,<sup>40</sup> and  $-0.05$  eV for  $\Delta G$  in the absence of alcohols. The CS process in the present ET system is in the Marcus normal region ( $\lambda > -\Delta G$ ). The alcohol concentration dependences of  $E_{1/2}^{\text{red}}$  and  $\lambda$  are calculated with eqs 7 and 9, respectively. The  $k_{\text{CS}}$  values are calculated by using eq 8 with the calculated alcohol concentration dependences of  $\Delta G$  and  $\lambda$ . As can be seen in Figures 3 and 5, the alcohol concentration dependences of  $k_{\text{CS}}$  and  $E_{1/2}^{\text{red}}$  are well reproduced by the same  $K$  and  $K^-$  values. The fitting parameters were  $K = 12$  (mol dm<sup>-3</sup>)<sup>-3</sup> and  $K^- = 300$  (mol dm<sup>-3</sup>)<sup>-3</sup> for MeOH and  $K \approx 0$  (mol dm<sup>-3</sup>)<sup>-1.2</sup> and  $K^- = 30$  (mol dm<sup>-3</sup>)<sup>-1.2</sup> for 1-PrOH. The  $\text{p}K_{\text{a}}$  values for the alcohols in water were reported to be 15.09 for MeOH, 15.93 for EtOH, and 16.1 for 1-PrOH, respectively.<sup>46</sup> In this  $\text{p}K_{\text{a}}$  range, the acidity of alcohols parallels the hydrogen bonding power.<sup>11</sup> The alcohols with the lower  $\text{p}K_{\text{a}}$  values have the stronger hydrogen bonding powers. The relative magnitudes of the chemical equilibrium constants (MeOH > EtOH > 1-PrOH) obtained in the present study were consistent with the order of the hydrogen bonding powers estimated from the  $\text{p}K_{\text{a}}$  values.

In the fitting of the experimental data, we approximately considered the single global equilibrium for the formation of the hydrogen bonding complex. This analysis gave the fractional  $n$  values, which seemed to be unnatural in view of the stoichiometry of the hydrogen bonding complexes. The single

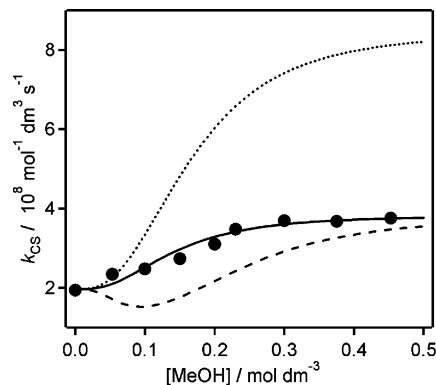


**Figure 7.** Plots of the rate constant ( $k_{\text{CS}}$ ) for the CS reaction in the <sup>3</sup>ZnTPP\*–DQ complex versus the concentration of MeOH calculated with the concerted pathway (solid line), stepwise pathway (dashed line), and a constant  $\lambda$  value (dotted line). The filled circles indicate the corresponding experimental results.

chemical equilibrium model used in the present study is phenomenological and does not give the precise physical significance. The fractional  $n$  values suggest a coexistence of several hydrogen bonding complexes with the different  $n$  numbers.<sup>14</sup> The obtained fractional  $n$  numbers correspond to averaged values for several hydrogen bonding complexes. The  $K$  values for the hydrogen bonding complex involving the neutral quinones have been obtained by the change of the UV absorption of quinones.<sup>12</sup> Since the solvent (PhCN) absorption is overlapped with that of DQ in the UV region, it is difficult to estimate the  $K$  value of DQ. Also, the calculated results were insensitive to the  $K$  value when the  $K$  value was smaller than 1. Though the value of  $K \approx 0$  (mol dm<sup>-3</sup>)<sup>- $n$</sup>  was used for the fitting of the experimental data obtained with EtOH and 1-PrOH, some amounts of DQ form hydrogen bonding with EtOH and 1-PrOH in the neutral state. We have roughly estimated that the  $K$  values for EtOH and for 1-PrOH were smaller than 1. From the above reasons, the  $K$  and  $K^-$  values used for fitting may contain some errors. Importantly, we could fit both of the alcohol concentration dependences of  $k_{\text{CS}}$  and  $E_{1/2}^{\text{red}}$  with the same parameter sets. This fact indicates that the alcohol concentration dependence of  $\lambda$  is given by the stabilization energies of the quinone anion due to the hydrogen bonding interactions, indicating that the CS reactions took place via the concerted pathway.

We also examined the other two possibilities for the hydrogen bonding effects on the CS reaction observed in the present study. The first possibility is that hydrogen bonding only stabilizes the charge separated state and does not affect  $\lambda$ . The MeOH concentration dependence of  $k_{\text{CS}}$  was calculated with a constant  $\lambda$  value and the alcohol concentration dependence of  $\Delta G$  estimated by eq 7. The second possibility is that the ET reaction takes place with the stepwise pathway. The alcohol concentration dependence of  $\Delta G$  was calculated by eq 7, while that of  $\lambda$  was calculated by eq 10. MeOH concentration dependences of  $k_{\text{CS}}$  calculated with a constant  $\lambda$  value and with the stepwise pathway are depicted in Figure 7 together with the calculations obtained with the concerted pathway. When the constant  $\lambda$  value was used in the calculation, the calculation overestimated the hydrogen bonding effects on  $k_{\text{CS}}$  and largely deviated from the experimental results. In the calculation with the stepwise pathway, the CS reaction was decelerated when the concentration of MeOH was lower than 0.2 mol dm<sup>-3</sup>. In this region, the increase in  $\lambda$  is larger than the stabilization energy of the charge separated state. This deceleration of  $k_{\text{CS}}$  with the addition of the alcohols also contradicts the experimental results. The

calculated results indicate that the observed alcohol concentration dependences of  $k_{CS}$  are associated with the concerted pathway, and eq 9 is validated to evaluate the hydrogen bonding effects on  $\lambda$  in the concerted pathway.

In the present study, the maxima for the increase of the  $\lambda$  value ranged from 0.05 to 0.1 eV. In the similar ET system, however, the increase in  $\lambda$  for the charge recombination was estimated to be 0.2 eV from the time-resolved EPR spectroscopy.<sup>23</sup> The increase in  $\lambda$  reported is larger than that obtained in the present study, though samples (quinone and alcohols), their concentrations, and solvent used in the time-resolved EPR measurements were nearly the same with that used in the present study. In the time-resolved EPR measurements, the singlet–triplet energy splitting ( $J$ ) for the radical ion pair<sup>47</sup> was detected from the observation of the electron spin polarization produced by the radical pair mechanism.<sup>48</sup> In the radical ion pairs,  $J$  is created by the electronic perturbation between the charge separated and ground states.<sup>47</sup> The sign of  $J$  is dependent on the relative magnitude of  $\lambda$  and  $\Delta G$  for the charge recombination. At the Marcus top regions for the charge recombination reactions found by the time-resolved EPR measurements, the  $\lambda$  were determined from the  $\Delta G$  for the charge recombination, which was obtained by the electrochemical measurements. Therefore, the ET reactions associated with the time-resolved EPR measurements may be faster than or comparable with the formation/dissociation of the hydrogen bonding complex. The increases in  $\lambda$  by 0.2 eV obtained with the time-resolved EPR spectroscopy are in reasonable agreement with the increase in  $\lambda$  calculated by eq 10 for the stepwise pathway.<sup>49</sup> The discrepancy between the hydrogen bonding effects on  $\lambda$  between the present study and the previous one reflects the difference of the ET pathway. The CS reactions investigated in the present study took place with the concerted pathway, whereas the charge recombination reactions observed in the previous time-resolved EPR study proceeded via the stepwise pathway. For both of the ET reactions, the observed increases in  $\lambda$  due to the hydrogen bonding interactions are described by the model proposed in the present study.

## Conclusion

The alcohol concentration dependences of the CS reaction between <sup>3</sup>ZnTPP\* and DQ in PhCN were studied by nanosecond laser flash photolysis. The observed CS reaction was accelerated with the additions of MeOH, EtOH, and 1-ProOH. The simple theory was developed to calculate the hydrogen bonding effects on  $\lambda$  for the concerted ET pathway and the stepwise one using the chemical equilibrium constants for the hydrogen bonding complexes. The theoretical results indicate that the  $\lambda$  value increases in the presence of the hydrogen bonding interactions for both pathways in addition to the stabilization of the charge separated state. The experimental results were analyzed by the classical Marcus equation where the hydrogen bonding effects on  $\lambda$  and  $\Delta G$  are calculated with the chemical equilibrium constants. The accelerations of the CS reactions observed in the presence of the alcohols are explained by the increase in  $\lambda$  and decrease in  $\Delta G$  due to the formation of the hydrogen bonding complexes and consistent with the ET reactions via the concerted pathway. The results provide valuable insights into the role of the hydrogen bonding interactions in biological ET systems where cofactor molecules are bounded through hydrogen bonding.

**Acknowledgment.** This work was partially supported by a Grant-in-Aid for Young Scientists (No. 21750009) from the Ministry of Education, Culture, Sports, Science and Technology of Japan.

## References and Notes

- (1) Hoff, A. J.; Deisenhofer, J. *Phys. Rep.* **1997**, *287*, 1–247.
- (2) Deisenhofer, J.; Norris, J. R., Eds. *The Photosynthetic Reaction Center*; Academic Press: San Diego, CA, 1993; Vols. 1–2.
- (3) (a) Möbius, K. *Chem. Soc. Rev.* **2000**, *29*, 129–139. (b) Möbius, K.; Savitsky, A.; Schnegg, A.; Plato, M.; Fuchs, M. *Phys. Chem. Chem. Phys.* **2005**, *7*, 19–42.
- (4) Brondijk, T. H. C.; van Boxel, G. I.; Mather, O. C.; Quirk, P. G.; White, S. A.; Jackson, J. B. *J. Biol. Chem.* **2006**, *281*, 13345–13354.
- (5) Yuasa, J.; Yamada, S.; Fukuzumi, S. *J. Am. Chem. Soc.* **2008**, *130*, 5808–5820.
- (6) Feher, G.; Allen, J. P.; Okamura, M. Y.; Rees, D. C. *Nature* **1989**, *339*, 111–116.
- (7) (a) Marcus, R. A. *J. Chem. Phys.* **1956**, *24*, 966–978. (b) Marcus, R. A. *J. Chem. Phys.* **1956**, *24*, 979–989.
- (8) Marcus, R. A.; Sutin, N. *Biochem. Biophys. Acta* **1985**, *811*, 265–322.
- (9) (a) Breinlinger, E.; Niemz, A.; Rotello, V. M. *J. Am. Chem. Soc.* **1995**, *117*, 5379–5380. (b) Niemz, A.; Rotello, V. M. *Acc. Chem. Res.* **1999**, *32*, 44–52.
- (10) (a) Ge, Y.; Lilienthal, R. R.; Smith, D. K. *J. Am. Chem. Soc.* **1996**, *118*, 3976–3977. (b) Ge, Y.; Miller, L.; Ouimet, T.; Smith, D. K. *J. Org. Chem.* **2000**, *65*, 8831–8838.
- (11) Gupta, N.; Linschitz, H. *J. Am. Chem. Soc.* **1997**, *119*, 6384–6391.
- (12) (a) Okumura, N.; Uno, B. *Bull. Chem. Soc. Jpn.* **1999**, *72*, 1213–1217. (b) Uno, B.; Okumura, N.; Goto, M.; Kano, K. *J. Org. Chem.* **2000**, *65*, 1448–1455.
- (13) Lehman, M. W.; Evans, D. H. *J. Phys. Chem. B* **2001**, *105*, 8877–8884.
- (14) Gómez, M.; González, F. I.; González, I. *Electroanalysis* **2003**, *15*, 635–645.
- (15) Bourgel, C.; Boyd, A. S. F.; Cooke, G.; de Cremiers, H. A.; Duclairoir, F. M. A.; Rottello, V. M. *Chem. Commun.* **2001**, 1954–1955.
- (16) Okamoto, K.; Ohkubo, K.; Kadish, K. M.; Fukuzumi, S. *J. Phys. Chem. A* **2004**, *108*, 10405–10413.
- (17) Sjödin, M.; Irebo, T.; Utas, J. E.; Lind, J.; Merényi, G.; Åkærmark, B.; Hammarström, L. *J. Am. Chem. Soc.* **2006**, *128*, 13076–13083.
- (18) Rhile, I. J.; Markle, T. F.; Nagano, H.; DiPasquale, A. G.; Lam, O. P.; Lockwood, M. A.; Rotter, K.; Mayer, J. M. *J. Am. Chem. Soc.* **2006**, *128*, 6075–6088.
- (19) Ishikita, H.; Soudackov, A. V.; Hammes-Schiffer, S. *J. Am. Chem. Soc.* **2007**, *129*, 11146–11152.
- (20) Huynh, M. H. V.; Meyer, T. J. *Chem. Rev.* **2007**, *107*, 5004–5064.
- (21) Hammes-Schiffer, S.; Soudackov, A. V. *J. Phys. Chem. B* **2008**, *112*, 14108–14123.
- (22) Reece, S. Y.; Nocera, D. G. *Annu. Rev. Biochem.* **2009**, *78*, 673–699.
- (23) (a) Kobori, Y.; Yago, T.; Akiyama, K.; Tero-Kubota, S. *J. Am. Chem. Soc.* **2001**, *123*, 9722–9723. (b) Yago, T.; Kobori, Y.; Akiyama, K.; Tero-Kubota, S. *J. Phys. Chem. B* **2002**, *106*, 10074–10081. (c) Yago, T.; Kobori, Y.; Akiyama, K.; Tero-Kubota, S. *Chem. Phys. Lett.* **2003**, *369*, 49–54.
- (24) VandeVondele, J.; Sulpizi, M.; Sprik, M. *Angew. Chem., Int. Ed.* **2006**, *45*, 1936–1938.
- (25) Caricato, M.; Ingrosso, F.; Mennucci, B.; Sato, H. *J. Phys. Chem. B* **2006**, *110*, 25115–25121.
- (26) Gohdo, M.; Kitahama, Y.; Sakaguchi, Y.; Wakasa, M. *J. Photochem. Photobiol., A* **2008**, *199*, 130–135.
- (27) Wakasa, M. *J. Phys. Chem. B* **2007**, *111*, 9434–9436.
- (28) Kobori, Y.; Yago, T.; Akiyama, K.; Tero-Kubota, S.; Sato, H.; Hirata, F.; Norris, J. R. *J. Phys. Chem. B* **2004**, *108*, 10226–10240.
- (29) Yonezawa, T.; Kawamura, T.; Ushio, M.; Nakano, Y. *Bull. Chem. Soc. Jpn.* **1970**, *43*, 1022–1027.
- (30) Kaupp, M.; Remenyi, C.; Vaara, J.; Malkina, O. L.; Malkin, V. G. *J. Am. Chem. Soc.* **2002**, *124*, 2709–2722.
- (31) Pekkarinen, L.; Linschitz, H. *J. Am. Chem. Soc.* **1960**, *82*, 2407–2411.
- (32) Kikuchi, K.; Kurabayashi, Y.; Kukubun, Y.; Kaizu, Y.; Kobayashi, H. *J. Photochem. Photobiol., A* **1988**, *45*, 261–263.
- (33) Görner, H. *Photochem. Photobiol.* **2003**, *78*, 440–448.
- (34) Chosrowjan, H.; Taniguchi, S.; Okada, T.; Takagi, S.; Arai, T.; Tokumaru, K. *Chem. Phys. Lett.* **1995**, *242*, 644–649.
- (35) Kavarnos, G. J.; Turro, N. J. *Chem. Rev.* **1986**, *86*, 401–449.
- (36) Riddick, J. A.; Bunger, W.; Sakano, T. K. *Organic Solvents*, 4th ed.; Wiley: New York, 1986.
- (37) Rehm, D.; Weller, A. *Isr. J. Chem.* **1970**, *8*, 259–271.

(38) Murov, S. L.; Carmichael, I.; Hug, G. L. *Handbook of Photochemistry*, 2nd ed.; Marcel Dekker: New York, 1993.

(39) Meites, L. *Polarographic Techniques*, 2nd ed.; John Wiley & Sons: New York, 1965.

(40) Yago, T.; Gohdo, M.; Wakasa, M. *Chem. Lett.* **2009**, 38, 880–881.

(41) In the normalized reaction coordinate, the equilibrium reaction coordinates for the reactant and product states are fixed to 0 and 1, respectively. When the reaction coordinate is defined as changes of the solute and solvent molecules such as chemical bond length and solvent molecule polarizations without normalization, reactant and product potential energy surfaces are shifted along the reaction coordinates by  $x$  different amounts because of the difference in the chemical equilibrium constants  $K$  and  $K^-$ .

(42) (a) Yago, T.; Kobori, Y.; Akiyama, K.; Tero-Kubota, S. *J. Phys. Chem. B* **2003**, 107, 13255–13257. (b) Yago, T.; Kobori, Y.; Akiyama, K.; Tero-Kubota, S. *Bull. Chem. Soc. Jpn.* **2004**, 77, 1997–2001.

(43) (a) Savéant, J.-M. *J. Phys. Chem. B* **2001**, 105, 8995–9001. (b) Savéant, J.-M. *J. Am. Chem. Soc.* **2008**, 130, 4732–4741.

(44) (a) Fukuzumi, S. *Prog. Inorg. Chem.* **2009**, 56, 49. (b) Okamoto, K.; Imahori, H.; Fukuzumi, S. *J. Am. Chem. Soc.* **2003**, 125, 7014–7021.

(45) Atkins, P. W. *Physical Chemistry*, 4th ed.; Oxford University Press: Oxford, U.K., 1990.

(46) Abraham, M. H.; Grellier, P. L.; Prior, D. V.; Duce, P. P.; Morris, J. J.; Taylor, P. J. *J. Chem. Soc., Perkin Trans. 2* **1989**, 699–711.

(47) (a) Sekiguchi, S.; Kobori, Y.; Akiyama, K.; Tero-Kubota, S. *J. Am. Chem. Soc.* **1998**, 120, 1325–1326. (b) Kobori, Y.; Sekiguchi, S.; Akiyama, K.; Tero-Kubota, S. *J. Phys. Chem. A* **1999**, 103, 5416–5424. (c) Kobori, Y.; Akiyama, K.; Tero-Kubota, S. *J. Chem. Phys.* **2000**, 113, 465–468. (d) Kobori, Y.; Yago, T.; Tero-Kubota, S. *Appl. Magn. Reson.* **2003**, 23, 269–287.

(48) (a) Adrian, F. J. *J. Chem. Phys.* **1971**, 54, 3918–3923. (b) Monchick, L.; Adrian, F. J. *J. Chem. Phys.* **1978**, 68, 4376–4383.

(49) This consideration may not be applied to the experimental observations obtained with MeOH. The  $k_{CS}$  value showed a rapid increase in the presence of 0.6 mol dm<sup>-3</sup> of MeOH and deviated from the fitting. This may be due to the selective solvation of MeOH for DQ<sup>-</sup>. The increase in  $\lambda$  observed in the presence of 0.62 mol dm<sup>-3</sup> of MeOH by the time-resolved EPR measurements could not be explained by the present model alone.

JP909927W